

# Energy conditions, traversable wormholes and dust shells

Francisco S. N. Lobo\*

*Centro de Astronomia e Astrofísica da Universidade de Lisboa,  
Campo Grande, Ed. C8 1749-016 Lisboa, Portugal*

Firstly, we review the pointwise and averaged energy conditions, the quantum inequality and the notion of the “volume integral quantifier”, which provides a measure of the “total amount” of energy condition violating matter. Secondly, we present a specific metric of a spherically symmetric traversable wormhole in the presence of a generic cosmological constant, verifying that the null and the averaged null energy conditions are violated, as was to be expected. Thirdly, a pressureless dust shell is constructed around the interior wormhole spacetime by matching the latter geometry to a unique vacuum exterior solution. In order to further minimize the usage of exotic matter, we then find regions where the surface energy density is positive, thereby satisfying all of the energy conditions at the junction surface. An equation governing the behavior of the radial pressure across the junction surface is also deduced. Lastly, taking advantage of the construction, specific dimensions of the wormhole, namely, the throat radius and the junction interface radius, and estimates of the total traversal time and maximum velocity of an observer journeying through the wormhole, are also found by imposing the traversability conditions.

PACS numbers: 04.20.-q, 04.20.Jb, 04.40.-b

## I. INTRODUCTION

Much interest has been aroused in wormholes since the Morris-Thorne article [1]. These act as tunnels from one region of spacetime to another, possibly through which observers may freely traverse. Wormhole physics is a specific example of solving the Einstein field equation in the reverse direction, namely, one first considers an interesting and exotic spacetime metric, then finds the matter source responsible for the respective geometry. In this manner, it was found that these traversable wormholes possess a peculiar property, namely exotic matter, involving a stress-energy tensor that violates the null energy condition [1, 2, 3]. In fact, they violate all the known pointwise energy conditions and averaged energy conditions, which are fundamental to the singularity theorems and theorems of classical black hole thermodynamics. The weak energy condition (WEC) assumes that the local energy density is positive and states that  $T_{\mu\nu}U^\mu U^\nu \geq 0$ , for all timelike vectors  $U^\mu$ , where  $T_{\mu\nu}$  is the stress energy tensor. By continuity, the WEC implies the null energy condition (NEC),  $T_{\mu\nu}k^\mu k^\nu \geq 0$ , where  $k^\mu$  is a null vector. Violations of the pointwise energy conditions led to the averaging of the energy conditions over timelike or null geodesics [4]. For instance, the averaged weak energy condition (AWEC) states that the integral of the energy density measured by a geodesic observer is non-negative, i.e.,  $\int T_{\mu\nu}U^\mu U^\nu d\tau \geq 0$ , where  $\tau$  is the observer’s proper time. Although classical forms of matter are believed to obey these energy conditions, it is a well-known fact that they are violated by certain quantum fields, amongst which we may refer to the Casimir effect.

Pioneering work by Ford in the late 1970’s on a new set of energy constraints [5], led to constraints on negative energy fluxes in 1991 [6]. These eventually culminated in the form of the Quantum Inequality (QI) applied to energy densities, which was introduced by Ford and Roman in 1995 [7]. The QI was proven directly from Quantum Field Theory, in four-dimensional Minkowski spacetime, for free quantized, massless scalar fields and takes the following form

$$\frac{\tau_0}{\pi} \int_{-\infty}^{+\infty} \frac{\langle T_{\mu\nu}U^\mu U^\nu \rangle}{\tau^2 + \tau_0^2} d\tau \geq -\frac{3}{32\pi^2\tau_0^4}, \quad (1)$$

in which,  $U^\mu$  is the tangent to a geodesic observer’s worldline;  $\tau$  is the observer’s proper time and  $\tau_0$  is a sampling time. The expectation value  $\langle \rangle$  is taken with respect to an arbitrary state  $|\Psi\rangle$ . Contrary to the averaged energy conditions, one does not average over the entire worldline of the observer, but weights the integral with a sampling function of characteristic width,  $\tau_0$ . The inequality limits the magnitude of the negative energy violations and the time for which they are allowed to exist.

The basic applications to curved spacetimes is that these appear flat if restricted to a sufficiently small region. The application of the QI to wormhole geometries is of particular interest [8]. A small spacetime volume around the throat of the wormhole was considered, so that all the dimensions of this volume are much smaller than the minimum proper radius of curvature in the

---

\*Electronic address: flobo@cosmo.fis.fc.ul.pt

region. Thus, the spacetime can be considered approximately flat in this region, so that the QI constraint may be applied. The results of the analysis is that either the wormhole possesses a throat size which is only slightly larger than the Planck length, or there are large discrepancies in the length scales which characterize the geometry of the wormhole. The analysis imply that generically the exotic matter is confined to an extremely thin band, and/or that large red-shifts are involved, which present severe difficulties for traversability, such as large tidal forces [8]. Due to these results, Ford and Roman concluded that the existence of macroscopic traversable wormholes is very improbable (see [9] for an interesting review). It was also shown that, by using the QI, enormous amounts of exotic matter are needed to support the Alcubierre warp drive and the superluminal Krasnikov tube [10, 11, 12]. However, there are a series of objections that can be applied to the QI. Firstly, the QI is only of interest if one is relying on quantum field theory to provide the exotic matter to support the wormhole throat. But there are classical systems (non-minimally coupled scalar fields) that violate the null and the weak energy conditions [13], whilst presenting plausible results when applying the QI. Secondly, even if one relies on quantum field theory to provide exotic matter, the QI does not rule out the existence of wormholes, although they do place serious constraints on the geometry. Thirdly, it may be possible to reformulate the QI in a more transparent covariant notation, and to prove it for arbitrary background geometries.

More recently, Visser *et al* [14, 15], noting the fact that the energy conditions do not actually quantify the “total amount” of energy condition violating matter, developed a suitable measure for quantifying this notion by introducing a “volume integral quantifier”. This notion amounts to calculating the definite integrals  $\int T_{\mu\nu}U^\mu U^\nu dV$  and  $\int T_{\mu\nu}k^\mu k^\nu dV$ , and the amount of violation is defined as the extent to which these integrals become negative. Although the null energy and averaged null energy conditions are always violated for wormhole spacetimes, Visser *et al* considered specific examples of spacetime geometries containing wormholes that are supported by arbitrarily small quantities of averaged null energy condition violating matter. It is also interesting to note that by using the “volume integral quantifier”, extremely stringent conditions were found on “warp drive” spacetimes, considering non-relativistic velocities of the bubble velocity [16].

As the violation of the energy conditions is a problematic issue, depending on one’s point of view [13], it is interesting to note that an elegant class of wormhole solutions minimizing the usage of exotic matter was constructed by Visser [17, 18] using the cut-and-paste technique, in which the exotic matter is concentrated at the wormhole throat. Using these thin-shell wormholes, a dynamic stability was analyzed, either by choosing specific surface equations of state [19, 20, 21], or by considering a linearized stability analysis around a static solution [22, 23, 24]. One may also construct wormhole solutions by matching an interior wormhole to an exterior vacuum solution, at a junction surface. In particular, a thin shell around a traversable wormhole, with a zero surface energy density was analyzed in [25], and with generic surface stresses in [26]. A similar analysis for the plane symmetric case, with a negative cosmological constant, is done in [27]. A general class of wormhole geometries with a cosmological constant and junction conditions was analyzed by DeBenedictis and Das [28], and further explored in higher dimensions [29].

A particularly simple, yet interestingly enough, case is that of a construction of a dust shell around a traversable wormhole. The null energy condition violation at the throat is necessary to maintain the wormhole open, although the averaged null energy condition violating matter can be made arbitrarily small [14, 15]. Thus, in order to further minimize the usage of exotic matter, one may impose that the surface stress energy tensor obeys the energy conditions at the junction surface. For a pressureless dust shell, one need only find the regions in which the surface energy density is non-negative, to determine the regions in which all of the energy conditions are satisfied.

The plan of this paper is as follows: In section II, we present a specific spacetime metric of a spherically symmetric traversable wormhole, in the presence of a generic cosmological constant, analyzing the respective mathematics of embedding. We verify that the null energy and the averaged null energy conditions are violated, as was to be expected. Using the “volume integral quantifier” and considering the specific example of the Ellis “drainhole”, we verify that the construction of this spacetime geometry can be made with arbitrarily small quantities of averaged null energy condition violating matter. In section III, we present the unique exterior vacuum solution. In section IV, we construct a pressureless dust shell around the interior wormhole spacetime, by matching the latter to the exterior vacuum solution. We also deduce an expression governing the behavior of the radial pressure across the junction surface. In section V, we find regions where the surface energy density is positive, thereby satisfying all of the energy conditions at the junction, in order to further minimize the usage of exotic matter. In section VI, specific dimensions of the wormhole, namely, the throat radius and the junction interface radius, and estimates of the total traversal time and maximum velocity of an observer journeying through the wormhole, are also found by imposing the traversability conditions. Finally, we conclude in section VII.

## II. INTERIOR WORMHOLE SOLUTION

Consider the following static and spherically symmetric line element (with  $G = c = 1$ )

$$ds^2 = -e^{2\Phi(r)} dt^2 + \left( \frac{\Lambda}{3} r^2 - \frac{m(r)}{r} \right)^{-1} dr^2 + r^2 (d\theta^2 + \sin^2 \theta d\phi^2), \quad (2)$$

where  $\Phi(r)$  and  $m(r)$  are arbitrary functions of the radial coordinate,  $r$ , and  $\Lambda$  is the cosmological constant.  $\Phi(r)$  is called the redshift function, for it is related to the gravitational redshift. We shall see ahead that this metric corresponds to a wormhole spacetime, so that  $m(r)$  can be denoted as the form function, as it determines the shape of the wormhole [1]. The radial coordinate has a range that increases from a minimum value at  $r_0$ , corresponding to the wormhole throat, to  $a$ , where the interior spacetime will be joined to an exterior vacuum solution.

Consider, without a significant loss of generality, an equatorial slice,  $\theta = \pi/2$ , of the line element (2), at a fixed moment of time and a fixed  $\phi$ . The metric is thus reduced to  $ds^2 = (\Lambda r^2/3 - m/r)^{-1} dr^2$ , which can then be embedded in a two-dimensional Euclidean space,  $ds^2 = dz^2 + dr^2$ . The lift function,  $z$ , is only a function of  $r$ , i.e.,  $z = z(r)$ . Thus, identifying the radial coordinate,  $r$ , of the embedding space with the slice considered of the wormhole geometry, we have the condition for the embedding surface, given by

$$\frac{dz}{dr} = \pm \left( \frac{1 - \frac{\Lambda}{3}r^2 + \frac{m}{r}}{\frac{\Lambda}{3}r^2 - \frac{m}{r}} \right)^{1/2}. \quad (3)$$

To be a solution of a wormhole, the radial coordinate has a minimum value,  $r = r_0$ , denoted as the throat, which defined in terms of the shape function is given by

$$m(r_0) = \frac{\Lambda}{3} r_0^3. \quad (4)$$

At this value the embedded surface is vertical, i.e.,  $dz/dr \rightarrow \infty$ . As in a general wormhole solution, the radial coordinate  $r$  is ill-behaved near the throat, but the proper radial distance,  $l(r) = \pm \int_{r_0}^r (\Lambda r'^2/3 - m(r')/r')^{-1/2} dr'$ , is required to be finite throughout spacetime. This implies that the condition  $\Lambda r'^2/3 - m(r')/r' \geq 0$  is imposed. Furthermore, one needs to impose that the throat flares out, which mathematically entails that the inverse of the embedding function,  $r(z)$ , must satisfy  $d^2r/dz^2 > 0$  at or near the throat. This flaring-out condition is given by

$$\frac{d^2r}{dz^2} = \frac{\frac{2\Lambda}{3}r^3 - m'r + m}{2 \left( r - \frac{\Lambda}{3}r^3 + m \right)^2} > 0, \quad (5)$$

implying that at the throat,  $r = r_0$  or  $m(r_0) = \Lambda r_0^3/3$ , we have the important condition

$$m'(r_0) < \Lambda r_0^2. \quad (6)$$

We will see below that this condition plays a fundamental role in the analysis of the violation of the energy conditions.

Using the Einstein field equation,  $G_{\hat{\mu}\hat{\nu}} + \Lambda g_{\hat{\mu}\hat{\nu}} = 8\pi T_{\hat{\mu}\hat{\nu}}$ , in an orthonormal reference frame with the following set of basis vectors

$$\mathbf{e}_{\hat{t}} = e^{-\Phi} \mathbf{e}_t, \quad \mathbf{e}_{\hat{r}} = (\Lambda r^2/3 - m/r)^{1/2} \mathbf{e}_r, \quad \mathbf{e}_{\hat{\theta}} = r^{-1} \mathbf{e}_\theta, \quad \mathbf{e}_{\hat{\phi}} = (r \sin \theta)^{-1} \mathbf{e}_\phi. \quad (7)$$

the stress energy tensor components of the metric (2) are given by

$$\rho(r) = \frac{1}{8\pi} \left( \frac{1+m'}{r^2} - 2\Lambda \right), \quad (8)$$

$$p_r(r) = \frac{1}{8\pi} \left[ -\frac{r+m}{r^3} + \frac{2\Phi'}{r} \left( \frac{\Lambda}{3}r^2 - \frac{m}{r} \right) + \frac{4\Lambda}{3} \right], \quad (9)$$

$$p_t(r) = \frac{1}{8\pi} \left[ \left( \frac{\Lambda}{3}r^2 - \frac{m}{r} \right) \left( \Phi'' + (\Phi')^2 + \frac{\Phi'}{r} \right) - \frac{(1+r\Phi')}{2r^3} \left( m'r - m - \frac{2\Lambda}{3}r^3 \right) + \Lambda \right]. \quad (10)$$

$\rho(r)$  is the energy density,  $p_r(r)$  is the radial pressure, and  $p_t(r)$  is the pressure measured in the lateral directions, orthogonal to the radial direction.

One may readily verify that the null energy condition (NEC) is violated at the wormhole throat. The NEC states that  $T_{\hat{\mu}\hat{\nu}}k^{\hat{\mu}}k^{\hat{\nu}} \geq 0$ , where  $k^{\hat{\mu}}$  is a null vector. In the orthonormal frame,  $k^{\hat{\mu}} = (1, 1, 0, 0)$ , we have

$$T_{\hat{\mu}\hat{\nu}}k^{\hat{\mu}}k^{\hat{\nu}} = \rho(r) + p_r(r) = \frac{1}{8\pi r^3} \left[ m'r - m - \frac{2\Lambda}{3}r^3 + 2r^2\Phi' \left( \frac{\Lambda}{3}r^2 - \frac{m}{r} \right) \right]. \quad (11)$$

Due to the flaring out condition of the throat deduced from the mathematics of embedding, i.e., Eq. (6), we verify that at the throat  $m(r_0) = \Lambda r_0/3$ , and due to the finiteness of  $\Phi(r)$ , from Eq. (11) we have  $T_{\hat{\mu}\hat{\nu}}k^{\hat{\mu}}k^{\hat{\nu}} < 0$ . Matter that violates the NEC is denoted as exotic matter.

In particular, one may consider a specific class of form functions that impose that Eq. (2) is asymptotically flat. This condition is reflected in the embedding diagram as  $dz/dr \rightarrow 0$  in the limit  $l \rightarrow \pm\infty$ , i.e.,  $\Lambda r^2/3 - m/r \rightarrow 1$  as  $l \rightarrow \pm\infty$ . In this case we verify that the averaged null energy condition (ANEC), defined as  $\int T_{\hat{\mu}\hat{\nu}} k^{\hat{\mu}} k^{\hat{\nu}} d\lambda \geq 0$ , is also violated.  $\lambda$  is an affine parameter along a radial null geodesic. Carrying out an identical computation as in [3], we have

$$\int T_{\hat{\mu}\hat{\nu}} k^{\hat{\mu}} k^{\hat{\nu}} d\lambda = -\frac{1}{4\pi} \int \frac{1}{r^2} e^{-\Phi} \sqrt{\frac{\Lambda}{3} r^2 - \frac{m(r)}{r}} dr < 0. \quad (12)$$

One may also consider the “volume integral quantifier”, as defined in [14, 15], which provides information about the “total amount” of ANEC violating matter in the spacetime. Taking into account Eq. (11) and performing an integration by parts, the volume integral quantifier is given by

$$\int (\rho + p_r) dV = - \int_{r_0}^{\infty} (\Lambda r^2 - m') \left[ \ln \left( \frac{e^{\Phi}}{\Lambda r^2/3 - m(r)/r} \right) \right] dr. \quad (13)$$

Consider, for simplicity, the Ellis “drainhole” solution [30] (also considered in [1, 31]), which corresponds to choosing a zero redshift function,  $\Phi = 0$ , and the following form function

$$m(r) = \frac{r_0^2 - r^2}{r} + \frac{\Lambda}{3} r^3. \quad (14)$$

Suppose now that the wormhole extends from the throat,  $r_0$ , to a radius situated at  $a$ . Evaluating the volume integral, one deduces

$$\int (\rho + p_r) dV = \frac{1}{a} \left[ (a^2 - r_0^2) \ln \left( 1 - \frac{r_0^2}{a^2} \right) + 2r_0(r_0 - a) \right]. \quad (15)$$

Taking the limit as  $a \rightarrow r_0^+$ , one verifies that  $\int (\rho + p_r) dV \rightarrow 0$ . Thus, as in the examples presented in [14, 15], with the form function of Eq. (14), one may construct a traversable wormhole with arbitrarily small quantities of ANEC violating matter. The exotic matter threading the wormhole extends from the throat at  $r_0$  to the junction boundary situated at  $a$ , where the interior solution is matched to an exterior vacuum spacetime.

### III. EXTERIOR VACUUM SOLUTION

In general, the solutions of the interior and exterior spacetimes are given in different coordinate systems. Therefore, to distinguish between both spacetimes, the exterior vacuum solution, written in the coordinate system  $(\bar{t}, \bar{r}, \bar{\theta}, \bar{\phi})$ , is given by

$$d\bar{s}^2 = - \left( 1 - \frac{2M}{\bar{r}} - \frac{\bar{\Lambda}}{3} \bar{r}^2 \right) d\bar{t}^2 + \left( 1 - \frac{2M}{\bar{r}} - \frac{\bar{\Lambda}}{3} \bar{r}^2 \right)^{-1} d\bar{r}^2 + \bar{r}^2 (d\bar{\theta}^2 + \sin^2 \bar{\theta} d\bar{\phi}^2). \quad (16)$$

If  $\bar{\Lambda} > 0$ , the solution is denoted by the Schwarzschild-de Sitter spacetime. For  $\bar{\Lambda} < 0$ , we have the Schwarzschild-anti de Sitter spacetime, and of course the specific case of  $\bar{\Lambda} = 0$  is reduced to the Schwarzschild solution, with a black hole event horizon at  $\bar{r}_b = 2M$ . Note that the metric (16) is asymptotically de Sitter, if  $\bar{\Lambda} > 0$  as  $\bar{r} \rightarrow \infty$ , or asymptotically anti-de Sitter, if  $\bar{\Lambda} < 0$ , as  $\bar{r} \rightarrow \infty$ .

For the Schwarzschild-de Sitter spacetime,  $\bar{\Lambda} > 0$ , if  $0 < 9\bar{\Lambda}M^2 < 1$ , then the factor  $f(\bar{r}) = 1 - 2M/\bar{r} - \bar{\Lambda}\bar{r}^2/3$  possesses two positive real roots (see [24, 25, 26] for details),  $\bar{r}_b$  and  $\bar{r}_c$ , corresponding to the black hole and the cosmological event horizons of the de Sitter spacetime, respectively. In this domain we have  $2M < \bar{r}_b < 3M$  and  $\bar{r}_c > 3M$ .

Considering the Schwarzschild-anti de Sitter metric, with  $\bar{\Lambda} < 0$ , the factor  $f(\bar{r})$  has only one real positive root,  $\bar{r}_b$ , corresponding to a black hole event horizon, with  $0 < \bar{r}_b < 2M$  (see [24, 25, 26] for details).

### IV. JUNCTION CONDITIONS

We shall match Eqs. (2) and (16) at a junction surface,  $S$ , situated at  $r = \bar{r} = a$ . In order for these line elements to be continuous across the junction,  $ds^2|_S = d\bar{s}^2|_S$ , we consider the following transformations

$$\bar{t} = \frac{t e^{\Phi(a)}}{\sqrt{1 - \Lambda a^2/3 - 2M/a}}, \quad (17)$$

$$\left. \frac{d\bar{r}}{dr} \right|_{r=a} = \frac{\sqrt{1 - \Lambda a^2/3 - 2M/a}}{\sqrt{\Lambda a^2/3 - m(a)/a}}, \quad (18)$$

$$\bar{\theta} = \theta \quad \text{and} \quad \bar{\phi} = \phi. \quad (19)$$

$\bar{\Lambda}$  and  $\Lambda$  correspond to the exterior and interior cosmological constants, respectively, which we shall assume continuous across the junction surface, i.e.,  $\bar{\Lambda} = \Lambda$ . We shall consider that the junction surface  $S$  is a timelike hypersurface defined by the parametric equation of the form  $f(x^\mu(\xi^i)) = 0$ .  $\xi^i = (\tau, \theta, \phi)$  are the intrinsic coordinates on  $S$ , and  $\tau$  is the proper time as measured by a comoving observer on the hypersurface. The intrinsic metric to  $S$  is given by

$$ds_S^2 = -d\tau^2 + a^2 (d\theta^2 + \sin^2 \theta d\phi^2). \quad (20)$$

Note that the junction surface,  $r = a$ , is situated outside the event horizon, i.e.,  $a > \bar{r}_b$ , to avoid a black hole solution.

Using the Darmois-Israel formalism [32, 33], the surface stresses at the junction interface are given by

$$\sigma = -\frac{1}{4\pi a} \left( \sqrt{1 - \frac{2M}{a} - \frac{\Lambda}{3}a^2} - \sqrt{\frac{\Lambda}{3}a^2 - \frac{m(a)}{a}} \right), \quad (21)$$

$$\mathcal{P} = \frac{1}{8\pi a} \left( \frac{1 - \frac{M}{a} - \frac{2\Lambda}{3}a^2}{\sqrt{1 - \frac{2M}{a} - \frac{\Lambda}{3}a^2}} - \zeta \sqrt{\frac{\Lambda}{3}a^2 - \frac{m(a)}{a}} \right), \quad (22)$$

with  $\zeta = 1 + a\Phi'(a)$  [26].  $\sigma$  and  $\mathcal{P}$  are the surface energy density and the tangential surface pressure, respectively. The surface mass of the thin shell is given by  $M_s = 4\pi a^2 \sigma$ . The total mass of the system,  $M$ , is provided by the following expression

$$M = \frac{a + m(a)}{2} - \frac{\Lambda}{3}a^3 + M_s \left( \sqrt{\frac{\Lambda}{3}a^2 - \frac{m(a)}{a}} - \frac{M_s}{2a} \right). \quad (23)$$

In particular, considering a pressureless dust shell,  $\mathcal{P} = 0$ , from Eq. (22), we have the following constraint

$$\zeta \sqrt{\frac{\Lambda}{3}a^2 - \frac{m(a)}{a}} = \frac{1 - \frac{M}{a} - \frac{2\Lambda}{3}a^2}{\sqrt{1 - \frac{2M}{a} - \frac{\Lambda}{3}a^2}}, \quad (24)$$

which restricts the values of the redshift parameter,  $\zeta$ . Eliminating the factor containing the form function in Eq. (21) by using Eq. (24), the surface energy density is then given by the following relationship

$$\sigma = \frac{1}{4\pi a \zeta} \left[ \frac{(1 - \zeta) + (\zeta - \frac{1}{2}) \frac{2M}{a} - (2 - \zeta) \frac{\Lambda}{3}a^2}{\sqrt{1 - \frac{2M}{a} - \frac{\Lambda}{3}a^2}} \right], \quad (25)$$

with  $\zeta \neq 0$ . This expression will be analyzed in the following section.

It is also of interest to obtain an equation governing the behavior of the radial pressure at the junction boundary in terms of the surface stresses at the junction boundary [3], given by

$$\begin{aligned} \bar{p}(a) - p(a) &= \frac{1}{a} \left( \sqrt{1 - \frac{2M}{a} - \frac{\Lambda}{3}a^2} + \sqrt{\frac{\Lambda}{3}a^2 - \frac{m(a)}{a}} \right) \mathcal{P} \\ &\quad - \left( \frac{\frac{M}{a^2} - \frac{\Lambda}{3}a}{\sqrt{1 - \frac{2M}{a} - \frac{\Lambda}{3}a^2}} + \Phi'(a) \sqrt{\frac{\Lambda}{3}a^2 - \frac{m(a)}{a}} \right) \frac{\sigma}{2}, \end{aligned} \quad (26)$$

where  $\bar{p}(a)$  and  $p(a)$  are the radial pressures acting on the shell from the exterior and the interior. Equation (26) relates the difference of the radial pressure across the shell in terms of a combination of the surface stresses,  $\sigma$  and  $\mathcal{P}$ , and the geometrical quantities. Note that  $\bar{p}(a) = 0$  for the exterior vacuum solution. Thus, for the particular case of a dust shell,  $\mathcal{P} = 0$ , Eq. (26) reduces to

$$p(a) = \frac{\sigma}{2a\zeta} \frac{[(\zeta - 1) + \frac{M}{a} - (3\zeta - 2) \frac{\Lambda}{3}a^2]}{\sqrt{1 - \frac{2M}{a} - \frac{\Lambda}{3}a^2}}. \quad (27)$$

## V. ENERGY CONDITIONS ON THE JUNCTION

The weak energy condition (WEC) on the junction surface implies  $\sigma \geq 0$  and  $\sigma + \mathcal{P} \geq 0$ , and by continuity implies the null energy condition (NEC),  $\sigma + \mathcal{P} \geq 0$ . The strong energy condition (SEC) at the junction surface reduces to  $\sigma + \mathcal{P} \geq 0$  and

$\sigma + 2\mathcal{P} \geq 0$ , and by continuity implies the NEC, but not necessarily the WEC. The dominant energy condition (DEC) implies  $\sigma \geq 0$  and  $\sigma \geq |\mathcal{P}|$ .

In principle, by taking the limit  $a \rightarrow r_0$  (note, however, that  $a > \bar{r}_b$ ), the “total amount” of the energy condition violating matter, of the interior solution, may be made arbitrarily small. Thus, in the spirit of further minimizing the usage of exotic matter, we shall find regions where the energy conditions are satisfied at the junction surface. For the specific case of a dust shell, this amounts to finding regions where  $\sigma \geq 0$  is satisfied. This shall be done for the Schwarzschild spacetime,  $\Lambda = 0$ , the Schwarzschild-de Sitter solution,  $\Lambda > 0$ , and the Schwarzschild-anti de Sitter spacetime,  $\Lambda < 0$ . In the analysis that follows we shall only be interested in positive values of  $M$ .

### A. Schwarzschild spacetime

For the Schwarzschild spacetime,  $\Lambda = 0$ , one needs to impose that  $m(r) < 0$ , so that Eq. (24) reduces to

$$\zeta \sqrt{\frac{|m(a)|}{a}} = \frac{1 - \frac{M}{a}}{\sqrt{1 - \frac{2M}{a}}}. \quad (28)$$

The right hand term is positive, which implies that the redshift parameter is always positive,  $\zeta > 0$ .

Equation (25) reduces to

$$\sigma = \frac{1}{4\pi a \zeta} \left[ \frac{(1 - \zeta) + (\zeta - \frac{1}{2}) \frac{2M}{a}}{\sqrt{1 - \frac{2M}{a}}} \right]. \quad (29)$$

To analyze this relationship, we shall define a new dimensionless parameter,  $\xi = 2M/a$ . Therefore, Eq. (29) may be rewritten in the following compact form

$$\sigma = \frac{1}{8\pi M} \frac{\Sigma(\xi, \zeta)}{\sqrt{1 - \xi}}, \quad (30)$$

with  $\Sigma(\xi, \zeta)$  given by

$$\Sigma(\xi, \zeta) = \frac{1}{\zeta} \left[ (1 - \zeta)\xi + \left( \zeta - \frac{1}{2} \right) \xi^2 \right]. \quad (31)$$

Equation (31) is depicted in Fig. 1. In the interval  $0 < \zeta \leq 1$ , we verify that  $\Sigma(\xi, \zeta) > 0$  for  $\forall \xi$ , implying a positive energy density,  $\sigma > 0$ , and thus satisfying all of the energy conditions.

For  $\zeta > 1$ , a boundary surface,  $\Sigma(\xi, \zeta) = 0$ , is given at  $\xi = (\zeta - 1)/(\zeta - 1/2)$ . A positive surface energy density is verified in the following region

$$\frac{\zeta - 1}{\zeta - \frac{1}{2}} \leq \xi < 1, \quad (32)$$

i.e.,  $2M < a < 2M(\zeta - 1/2)/(\zeta - 1)$ .

### B. Schwarzschild-de Sitter spacetime

For the Schwarzschild-de Sitter spacetime,  $\Lambda > 0$ , consider the definitions of the dimensionless parameters  $\beta = 9\Lambda M^2$  and  $\xi = 2M/a$ . Then Eq. (24) takes the form

$$\zeta \sqrt{\frac{\frac{\Lambda}{3}a^2 - m(a)}{a}} = \frac{1 - \frac{\xi}{2} - \frac{8\beta}{27\xi^2}}{\sqrt{1 - \xi - \frac{4\beta}{27\xi^2}}}. \quad (33)$$

We verify that the redshift parameter is null,  $\zeta = 0$ , if the factor  $f(\xi, \beta) = 1 - \frac{\xi}{2} - \frac{8\beta}{27\xi^2}$  is zero, i.e.,  $\beta_n = 27\xi^2(1 - \xi/2)/8$ , which is represented in Fig. 2. For  $\zeta > 0$ , we have  $f(\xi, \beta) > 0$ , or  $\beta < \beta_n$ ; for  $\zeta < 0$ , we have  $f(\xi, \beta) < 0$ , or  $\beta > \beta_n$ . Only the region below the solid curve, given by  $\beta_r = 27\xi^2(1 - \xi)/4$  is of interest.

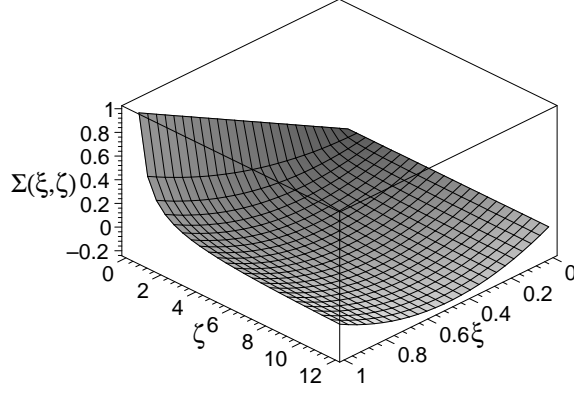


FIG. 1: Plot representing the sign of the surface energy density. The surface is given by Eq. (31). We have considered the definition  $\xi = 2M/a$ . For  $0 < \zeta \leq 1$  and  $\forall \xi$ , we verify that  $\Sigma(\xi, \zeta) > 0$ . For  $\zeta > 1$ , with  $\xi = (\zeta - 1)/(\zeta - 1/2)$ , we have  $\Sigma(\xi, \zeta) > 0$ . See text for details.

The surface energy density, Eq. (25), as in the previous case, may be rewritten in the following compact form

$$\sigma = \frac{1}{8\pi M} \frac{\Sigma(\xi, \zeta, \beta)}{\sqrt{1 - \xi - \frac{4\beta}{27\xi^2}}}, \quad (34)$$

with  $\Sigma(\xi, \zeta, \beta)$  given by

$$\Sigma(\xi, \zeta, \beta) = \frac{1}{\zeta} \left[ (1 - \zeta)\xi + (\zeta - 1/2)\xi^2 - (2 - \zeta)\frac{4\beta}{27\xi} \right], \quad (35)$$

with  $\zeta \neq 0$ .

To analyze Eq. (35) consider a null surface energy density,  $\sigma = 0$ , i.e.,  $\Sigma(\xi, \zeta, \beta) = 0$ , so that we deduce the relationship

$$\beta_0 = \frac{27}{4} \frac{\xi^2}{(2 - \zeta)} \left[ (1 - \zeta) + \left( \zeta - \frac{1}{2} \right) \xi \right], \quad (36)$$

for  $\zeta \neq 2$ . For the particular case of  $\zeta = 2$ , depicted in Fig. 2, Eq. (35) reduces to  $\Sigma(\xi, \zeta = 2, \beta) = (3\xi/2 - 1)\xi/2$ , which is null for  $\xi = 2/3$ , i.e.,  $a = 3M$ ; positive for  $\xi > 2/3$ , i.e.,  $r_b < a < 3M$ ; and negative for  $\xi < 2/3$ , i.e.,  $3M < a < r_c$ . Thus the energy conditions are satisfied in the region to the right of the curve,  $\zeta = 2$ , depicted in Fig. 2.

In the interval,  $0 < \zeta < 2$ , we verify that  $\Sigma(\xi, \zeta, \beta) \geq 0$ , for  $\beta \leq \beta_0$ . For  $\zeta > 2$ , then a non-negative surface energy density is verified for  $\beta \geq \beta_0$ . The particular case of  $\zeta = 3$  is depicted in Fig. 2. The energy conditions are also satisfied to the right of the respective curve and to the left of the solid line,  $\beta_r$ .

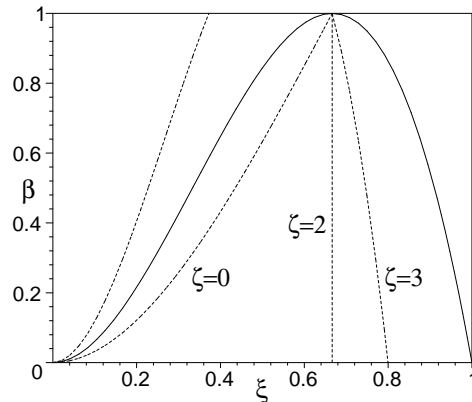


FIG. 2: Analysis of the energy conditions for the Schwarzschild-de Sitter spacetime. We have considered the definitions  $\beta = 9\Lambda M^2$  and  $\xi = 2M/a$ . Only the region below the solid line is of interest. The energy conditions are obeyed to the right of each respective dashed curves,  $\zeta = 0$ ,  $\zeta = 2$  and  $\zeta = 3$ . See text for details.

### C. Schwarzschild-anti de Sitter spacetime

For the Schwarzschild-anti de Sitter spacetime,  $\Lambda < 0$ , consider the parameters  $\kappa = 9|\Lambda|M^2$  and  $\xi = 2M/a$ . Then Eq. (24) takes the form

$$\zeta \sqrt{\frac{\Lambda}{3}a^2 - \frac{m(a)}{a}} = \frac{1 - \frac{\xi}{2} + \frac{4\kappa}{27\xi^2}}{\sqrt{1 - \xi + \frac{4\kappa}{27\xi^2}}}. \quad (37)$$

The right hand side of Eq. (37) is always positive, so that the restriction  $\zeta > 0$  is imposed.

The surface energy density, Eq. (25), is given in the following compact form

$$\sigma = \frac{1}{8\pi M} \frac{\Sigma(\xi, \zeta, \kappa)}{\sqrt{1 - \xi + \frac{4\kappa}{27\xi^2}}}, \quad (38)$$

with  $\Sigma(\xi, \zeta, \kappa)$  given by

$$\Sigma(\xi, \zeta, \kappa) = \frac{1}{\zeta} \left[ (1 - \zeta)\xi + (\zeta - 1/2)\xi^2 + (2 - \zeta)\frac{4\kappa}{27\xi} \right]. \quad (39)$$

Consider a null surface energy density,  $\sigma = 0$ , i.e.,  $\Sigma(\xi, \zeta, \kappa) = 0$ , so that from Eq. (39), we have the relationship

$$\kappa_0 = \frac{27}{4} \frac{\xi^2}{(2 - \zeta)} \left[ (\zeta - 1) - \left( \zeta - \frac{1}{2} \right) \xi \right], \quad (40)$$

for  $\zeta \neq 2$ . For the particular case of  $\zeta = 2$ , Eq. (39) takes the form  $\Sigma(\xi, \zeta = 2, \kappa) = (1 - 3\xi/2)\xi/2$ , which is null for  $\xi = 2/3$ , i.e.,  $a = 3M$ ; positive for  $\xi > 2/3$ , i.e.,  $r_b < a < 3M$ ; and negative for  $\xi < 2/3$ , i.e.,  $a > 3M$ . Only the region to the left of the solid curve, given by  $\kappa_r = 27\xi^2(\xi - 1)/4$ , is of interest.

For  $0 < \zeta \leq 1$ , a non-negative surface energy density is given for  $\forall \kappa$  and  $\forall \xi$ . For  $1 < \zeta < 2$ ,  $\Sigma(\xi, \zeta, \kappa) > 0$  for  $\kappa > \kappa_0$ . For  $\zeta > 2$ , we have  $\Sigma(\xi, \zeta, \kappa) > 0$  for  $\kappa_r < \kappa < \kappa_0$ .

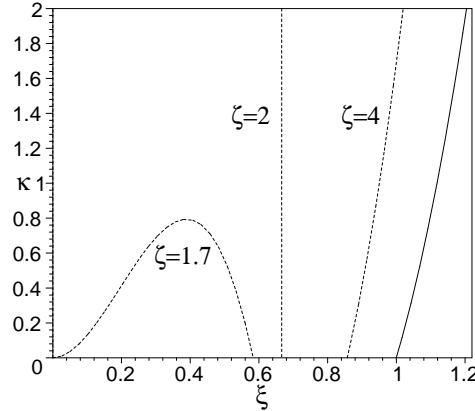


FIG. 3: Analysis of the energy conditions for the Schwarzschild-anti de Sitter spacetime. We have considered the definitions  $\kappa = 9|\Lambda|M^2$  and  $\xi = 2M/a$ . Only the region to the left of the solid curve, given by  $\kappa_r = 27\xi^2(\xi - 1)/4$ , is of interest. For the cases of  $\zeta = 2$  and  $\zeta = 4$ , the energy conditions are satisfied to the right of the respective dashed curves, and to the left of the solid line. For the specific case of  $\zeta = 1.7$ , the energy conditions are obeyed above the respective curve. See text for details.

### VI. TRAVERSABILITY CONDITIONS

In this section we shall consider the traversability conditions required for the traversal of a human being through the wormhole, and consequently determine specific dimensions for the wormhole. Specific cases for the traversal time and velocity will also be estimated. In this section we shall insert  $c$  to aid us in the computations.



Consider the redshift function given by  $\Phi(r) = kr^\alpha$ , with  $\alpha, k \in \mathbb{R}$ . Thus, from the definition of  $\zeta = 1 + a\Phi'(a)$ , the redshift function, in terms of  $\zeta$ , takes the following form

$$\Phi(r) = \frac{\zeta - 1}{\alpha} \left(\frac{r}{a}\right)^\alpha, \quad (41)$$

with  $\alpha \neq 0$ . With this choice of  $\Phi(r)$ ,  $\zeta$  may also be defined as  $\zeta = 1 + \alpha\Phi(a)$ . The case of  $\alpha = 0$  corresponds to the constant redshift function, so that  $\zeta = 1$ . If  $\alpha < 0$ , then  $\Phi(r)$  is finite throughout spacetime and in the absence of an exterior solution we have  $\lim_{r \rightarrow \infty} \Phi(r) \rightarrow 0$ . As we are considering a matching of an interior solution with an exterior solution at  $a$ , then it is also possible to consider the  $\alpha > 0$  case, imposing that  $\Phi(r)$  is finite in the interval  $r_0 \leq r \leq a$ .

One of the traversability conditions required is that the acceleration felt by the traveller should not exceed Earth's gravity [1]. Consider an orthonormal basis of the traveller's proper reference frame,  $(\mathbf{e}_{\hat{0}'}, \mathbf{e}_{\hat{1}'}, \mathbf{e}_{\hat{2}'}, \mathbf{e}_{\hat{3}'})$ , given in terms of the orthonormal basis vectors of Eqs. (7) of the static observers, by a Lorentz transformation, i.e.,

$$\mathbf{e}_{\hat{0}'} = \gamma \mathbf{e}_{\hat{t}} \mp \gamma v \mathbf{e}_{\hat{r}}, \quad \mathbf{e}_{\hat{1}'} = \mp \gamma \mathbf{e}_{\hat{r}} + \gamma v \mathbf{e}_{\hat{t}}, \quad \mathbf{e}_{\hat{2}'} = \mathbf{e}_{\hat{\theta}}, \quad \mathbf{e}_{\hat{3}'} = \mathbf{e}_{\hat{\phi}}, \quad (42)$$

where  $\gamma = (1 - v^2)^{-1/2}$ , and  $v(r)$  being the velocity of the traveller as he/she passes  $r$ , as measured by a static observer positioned there [1]. Thus, the traveller's four-acceleration expressed in his proper reference frame,  $\mathcal{A}^{\hat{\mu}'} = U^{\hat{\nu}'} U^{\hat{\mu}'}_{;\hat{\nu}'}$ , yields the following restriction

$$\left| \left( \frac{\Lambda}{3} r^2 - \frac{m(r)}{r} \right)^{1/2} e^{-\Phi} (\gamma e^\Phi)' c^2 \right| \leq g_\oplus, \quad (43)$$

The condition is immediately satisfied at the throat,  $m(r_0) = \Lambda r_0^3/3$ . From Eq. (43), one may also find an estimate for the junction surface,  $a$ . Consider that the dust shell is placed in an asymptotically flat region of spacetime, so that  $(\Lambda a^2/3 - m(a)/a)^{1/2} \approx 1$ . We also assume that the traversal velocity is constant,  $v = \text{const}$ , and non-relativistic,  $\gamma \approx 1$ . Taking into account Eq. (41), from Eq. (43) one deduces  $a \geq |\zeta - 1|c^2/g_\oplus$ . Considering the equality case, one has

$$a = \frac{|\zeta - 1|c^2}{g_\oplus}. \quad (44)$$

Providing a value for  $|\zeta - 1|$ , one may find an estimate for  $a$ . For instance, considering that  $|\zeta - 1| \simeq 10^{-10}$ , one finds that  $a \approx 10^6 \text{ m}$ .

Another of the traversability conditions required is that the tidal accelerations felt by the traveller should not exceed the Earth's gravitational acceleration [1]. The tidal acceleration felt by the traveller is given by  $\Delta \mathcal{A}^{\hat{\mu}'} = -R^{\hat{\mu}'}_{\hat{\nu}'\hat{\alpha}'\hat{\beta}'} U^{\hat{\nu}'} \eta^{\hat{\alpha}'} U^{\hat{\beta}'} c^2$ , where  $U^{\hat{\mu}'} = \delta^{\hat{\mu}'}_{\hat{0}'}$  is the traveller's four velocity and  $\eta^{\hat{\alpha}'}$  is the separation between two arbitrary parts of his body. Note that  $\eta^{\hat{\alpha}'}$  is purely spatial in the traveller's reference frame, as  $U^{\hat{\alpha}'} \eta_{\hat{\alpha}'} = 0$ , so that  $\eta^{\hat{0}'} = 0$ . For simplicity, assume that  $|\eta^{\hat{i}'}| \approx 2 \text{ m}$  along any spatial direction in the traveller's reference frame [1]. Thus, the constraint  $|\Delta \mathcal{A}^{\hat{\mu}'}| \leq g_\oplus$  provides the following inequalities

$$\left| \left( \frac{\Lambda}{3} r^2 - \frac{m}{r} \right) [\Phi'' + (\Phi')^2] - \frac{\Phi'}{2r^2} \left( m'r - m - \frac{2\Lambda}{3} r^3 \right) \right| |\eta^{\hat{1}'}| c^2 \leq g_\oplus, \quad (45)$$

$$\left| \frac{\gamma^2}{2r^3} \left[ \left( \frac{v}{c} \right)^2 \left( m'r - m - \frac{2\Lambda}{3} r^3 \right) + 2r^2 \left( \frac{\Lambda}{3} r^2 - \frac{m}{r} \right) \Phi' \right] \right| |\eta^{\hat{2}'}| c^2 \leq g_\oplus. \quad (46)$$

The radial tidal constraint, Eq. (45), constrains the redshift function, and the lateral tidal constraint, Eq. (46), constrains the velocity with which observers traverse the wormhole. At the throat,  $r = r_0$  or  $m(r_0) = \Lambda r_0^3/3$ , and taking into account Eq. (41), we verify that Eq. (45) reduces to  $|\eta^{\hat{1}'}| c^2 (m' - \Lambda r_0^2) \Phi'(r_0)/2r_0 \leq g_\oplus$  or

$$\left| \frac{(m' - \Lambda r_0^2)(\zeta - 1)}{2r_0^2} \left( \frac{r_0}{a} \right)^\alpha \right| = \frac{g_\oplus}{|\eta^{\hat{1}'}| c^2}, \quad (47)$$

considering the equality case. From this relationship, one may find estimates for the junction interface radius,  $a$ , and the wormhole throat,  $r_0$ . From Eq. (47), one deduces

$$a = \left( \frac{|m' - \Lambda r_0^2| |\zeta - 1| |\eta^{\hat{1}'}| c^2}{2g_\oplus r_0^2} \right)^{1/\alpha} r_0. \quad (48)$$

Using Eqs. (44) and (48), one may find an estimate for the throat radius, by providing a specific value for  $\alpha$ . For instance, considering  $\alpha = -1$  and equating Eqs. (44) and (48), one finds

$$r_0 = \left( \frac{|m' - \Lambda r_0^2| |\zeta - 1|^2 |\eta^{\hat{1}'}| c^4}{2g_\oplus^2} \right)^{1/3}. \quad (49)$$

Taking into account Eq. (6), if  $m'(r_0) \approx \Lambda r_0^2$ , we verify that the embedding diagram flares out very slowly, so that from Eq. (49),  $r_0$  may be made arbitrarily small. Nevertheless, using specific examples of the form function, for instance Eq. (14), we will assume the approximation  $|m' - \Lambda r_0^2| \approx 1$ . Using the above value of  $|\zeta - 1| = 10^{-10}$ , from Eq. (49) we find  $r_0 \simeq 10^4$  m.

One may use the lateral tidal constraint, Eq. (46), to find an upper limit of the traversal velocity,  $v$ . Evaluated at  $r_0$ , we find

$$v \leq \sqrt{\frac{2g_\oplus}{|m' - \Lambda r_0^2| |\eta^{\hat{2}'}|}} r_0. \quad (50)$$

Taking into account the values and approximations considered above, we have the upper bound of  $v \lesssim 3 \times 10^4$  m/s.

The traversal times as measured by the traveller and an observer situated at a space station, which we shall assume rests just outside the junction surface, are given respectively by [1]

$$\Delta\tau = \int_{-a}^a \frac{dl}{v\gamma} \quad \text{and} \quad \Delta t = \int_{-a}^a \frac{dl}{ve^\Phi}, \quad (51)$$

where  $dl = (\Lambda r^2/3 - m/r)^{-1/2} dr$  is the proper radial distance. Since we have chosen  $\gamma \approx 1$  and  $|\zeta - 1| \approx 10^{-10}$ , we can use the following approximations

$$\Delta\tau \approx \Delta t \approx \int_{-a}^a \frac{dl}{v} \approx \frac{2a}{v}. \quad (52)$$

For instance, considering the maximum velocity,  $v \approx 3 \times 10^4$  m/s, with  $a \approx 10^6$  m, the traversal through the wormhole can be made in approximately a minute.

## VII. CONCLUSION

We have presented a specific metric of a spherically symmetric traversable wormhole in the presence of a generic cosmological constant, verifying that the null energy condition and the averaged null energy condition are violated, as was to be expected. We verified that evaluating the “volume integral quantifier”, the specific Ellis drainhole may also be theoretically constructed with arbitrarily small quantities of averaged null energy condition violating matter. Furthermore, we constructed a pressureless dust shell around the interior wormhole solution, by matching the latter to a unique vacuum exterior spacetime, in the presence of a generic cosmological constant. In the spirit of minimizing the usage of exotic matter, regions were determined in which the surface energy density is non-negative, thus satisfying all of the energy conditions at the junction surface. An equation governing the behavior of the radial pressure across the shell was also determined. Taking advantage of the construction, and considering the traversability conditions, estimates of the throat radius and the junction interface radius, of the total traversal time and maximum velocity of an observer journeying through the wormhole, were also found.

- 
- [1] M. Morris and K. S. Thorne, “Wormholes in spacetime and their use for interstellar travel: A tool for teaching General Relativity”, Am. J. Phys. **56**, 395 (1988).
  - [2] M. Morris, K. S. Thorne and U. Yurtsever, “Wormholes, time machines and the weak energy condition”, Phys. Rev. Lett. **61**, 1442 (1988).
  - [3] M. Visser, *Lorentzian Wormholes: From Einstein to Hawking* (American Institute of Physics, New York, 1995).
  - [4] F. Tipler, “Energy conditions and spacetime singularities”, Phys. Rev. D **17**, 2521 (1978).
  - [5] L. H. Ford, Proc. Roy. Soc. Lond. **A 364**, 227 (1978).
  - [6] L. H. Ford, “Constraints on negative-energy fluxes”, Phys. Rev. D **43**, 3972 (1991).
  - [7] L. H. Ford and T. A. Roman, “Averaged energy conditions and quantum inequalities”, Phys. Rev. D **51**, 4277 (1995) [arXiv:gr-qc/9410043].
  - [8] L. H. Ford and T. A. Roman, “Quantum field theory constrains traversable wormhole geometries”, Phys. Rev. D **53**, 5496 (1996) [arXiv:gr-qc/9510071].

- [9] T. A. Roman, “Some Thoughts on Energy Conditions and Wormholes”, [arXiv:gr-qc/0409090].
- [10] M. J. Pfenning and L. H. Ford, “The unphysical nature of warp drive”, *Class. Quant. Grav.* **14**, 1743, (1997) [arXiv:gr-qc/9702026].
- [11] A. Everett and T.A. Roman, “A Superluminal Subway: The Krasnikov Tube”, *Phys. Rev. D* **56**, 2100 (1997) [arXiv:gr-qc/9702049].
- [12] For a review article, see for example:  
F. Lobo and P. Crawford, “Weak energy condition violation and superluminal travel”, *Current Trends in Relativistic Astrophysics, Theoretical, Numerical, Observational, Lecture Notes in Physics* **617**, Springer-Verlag Publishers, L. Fernández et al. eds, pp. 277–291 (2003) [arXiv:gr-qc/0204038].
- [13] C. Barcelo and M. Visser, “Scalar fields, energy conditions, and traversable wormholes,” *Class. Quant. Grav.* **17**, 3843 (2000) [arXiv:gr-qc/0003025].
- [14] M. Visser, S. Kar and N. Dadhich, “Traversable wormholes with arbitrarily small energy condition violations”, *Phys. Rev. Lett.* **90**, 201102 (2003) [arXiv:gr-qc/0301003].
- [15] S. Kar and N. Dadhich and M. Visser, “Quantifying energy condition violations in traversable wormholes”, *Pramana* (in press) [arXiv:gr-qc/0405103].
- [16] F. S. N. Lobo and M. Visser, “Fundamental limitations on “warp drive” spacetimes”, [arXiv:gr-qc/0406083].
- [17] M. Visser, “Traversable wormholes: Some simple examples”, *Phys. Rev. D* **39** 3182 (1989).
- [18] M. Visser, “Traversable wormholes from surgically modified Schwarzschild spacetimes”, *Nucl. Phys. B* **328** 203 (1989).
- [19] S. W. Kim, “Schwarzschild-de Sitter type wormhole”, *Phys. Lett. A* **166**, 13 (1992).
- [20] M. Visser, “Quantum mechanical stabilization of Minkowski signature”, *Phys. Lett. B* **242**, 24 (1990).
- [21] S. W. Kim, H. Lee, S. K. Kim and J. Yang, “(2 + 1)-dimensional Schwarzschild-de Sitter wormhole”, *Phys. Lett. A* **183**, 359 (1993).
- [22] E. Poisson and M. Visser, “Thin-shell wormholes: Linearization stability”, *Phys. Rev. D* **52** 7318 (1995) [arXiv:gr-qc/9506083].
- [23] E. F. Eiroa and G. E. Romero “Linearized stability of charged thin-shell wormholes”, *Gen. Rel. Grav.* **36** 651-659 (2004) [arXiv:gr-qc/0303093].
- [24] F. S. N. Lobo and P. Crawford, “Linearized stability analysis of thin-shell wormholes with a cosmological constant”, *Class. Quant. Grav.* **21**, 391 (2004) [arXiv:gr-qc/0311002].
- [25] J. P. S. Lemos, F. S. N. Lobo and S. Q. de Oliveira, “Morris-Thorne wormholes with a cosmological constant”, *Phys. Rev. D* **68**, 064004 (2003) [arXiv:gr-qc/0302049].
- [26] F. S. N. Lobo, “Surface stresses on a thin shell surrounding a traversable wormhole”, *Class. Quant. Grav.* **21** 4811 (2004) [arXiv:gr-qc/0409018].
- [27] J. P. S. Lemos and F. S. N. Lobo, “Plane symmetric traversable wormholes in an anti-de Sitter background”, *Phys. Rev. D* **69**, 104007 (2004) [arXiv:gr-qc/0402099].
- [28] A. DeBenedictis and A. Das, “On a General Class of Wormhole Geometries”, *Class. Quant. Grav.* **18** 1187 (2001) [gr-qc/0009072].
- [29] A. DeBenedictis and A. Das, “Higher Dimensional Wormhole Geometries with Compact Dimensions”, *Nucl. Phys. B* **653** 279 (2003) [arXiv:gr-qc/0207077].
- [30] H. G. Ellis, “Ether flow through a drainhole: A particle model in general relativity”, *J. Math. Phys.* **14**, 104 (1973).
- [31] E. G. Harris, “Wormhole connecting two Reissner-Nordström universes”, *Am. J. Phys.* **61**, 1140 (1993).
- [32] G. Darrois, “Mémoire des sciences mathématiques XXV”, Fascicule XXV ch V (Gauthier-Villars, Paris, France, 1927).
- [33] W. Israel, “Singular hypersurfaces and thin shells in general relativity”, *Nuovo Cimento* **44B**, 1 (1966); and corrections in *ibid.* **48B**, 463 (1966).